

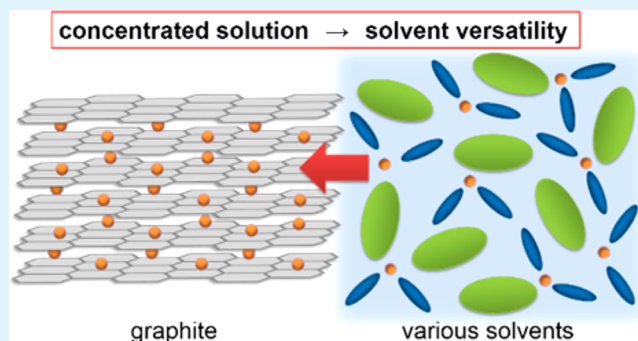
# General Observation of Lithium Intercalation into Graphite in Ethylene-Carbonate-Free Superconcentrated Electrolytes

Yuki Yamada, Kenji Usui, Ching Hua Chiang, Keisuke Kikuchi, Keizo Furukawa, and Atsuo Yamada\*

Department of Chemical System Engineering, The University of Tokyo, Tokyo 113-8656, Japan

**ABSTRACT:** Lithium-ion batteries have exclusively employed an ethylene carbonate (EC)-based electrolyte to ensure the reversibility of the graphite negative electrode reaction. Because of the limitation of electrolyte compositions, there has been no remarkable progress in commercial lithium-ion batteries despite active research on positive electrode materials. Herein, we present a salt-superconcentrating strategy as a simple and effective method of universalizing a graphite negative electrode reaction in various organic solvents. A dilute electrolyte (e.g.,  $1 \text{ mol dm}^{-3}$ ) of sulfoxide, ether, and sulfone results in solvent cointercalation and/or severe electrolyte decomposition at a graphite electrode, whereas their superconcentrated electrolyte (e.g.,  $>3 \text{ mol dm}^{-3}$ ) allows for highly reversible lithium intercalation into graphite. We have found a unique coordination structure in the superconcentrated solution and an anion-based inorganic SEI film on the cycled graphite electrode, which would be the origin of the reversible graphite negative electrode reaction without EC. Our salt-superconcentrating strategy, expanding the graphite negative electrode reaction in various organic solvents other than EC, will contribute to the development of advanced lithium-ion batteries with high-voltage and fast-charging characters based on new EC-free functional electrolytes.

**KEYWORDS:** lithium-ion batteries, electrolyte, negative electrode, graphite, concentrated solution, surface film



## INTRODUCTION

With heightened global interest in environmental and energy issues, electrochemical energy storage in a form of battery is getting much more attention as a key technology to realize a sustainable society with electric vehicles and smart grids based on natural energy.<sup>1,2</sup> A major requirement for large-scale batteries is high energy density (i.e., high voltage and large capacity) with retaining a high level of safety. A short-term strategy toward high energy density is realizing higher-voltage operation of lithium-ion batteries with a 5 V class positive electrode material.<sup>3</sup> For a long-term solution, large-capacity lithium–oxygen and lithium–sulfur batteries are currently studied as a post lithium-ion batteries.<sup>4</sup> A common technical challenge in realizing such advanced batteries is to develop a stable, functional electrolyte that allows for highly reversible positive/negative electrode reactions without suffering from severe oxidative/reductive decompositions. Specifically, high chemical/electrochemical stability (wide electrochemical window), fast ion-transport property, and high safety are required for the electrolyte in advanced batteries.

A nonaqueous organic electrolyte, consisting of an organic solvent and a lithium salt, has been widely used for batteries that deliver higher voltage than the electrochemical window of water (1.23 V). In pursuit of much higher stability and safety, room-temperature ionic liquids have been in the spotlight for decades due to their negligible volatility and low flammability as well as wide electrochemical window.<sup>5–7</sup> However, they have

an inherent problem in ionic transport property;  $\text{Li}^+$  transference number in ionic liquids is essentially low (e.g., 0.1–0.2)<sup>8</sup> because of the presence of reaction-irrelevant organic cations. Inorganic solid electrolytes have also been extensively studied because of their extremely high safety.<sup>9–11</sup> Although some of them exhibit even higher ionic conductivity than conventional organic electrolytes,<sup>9</sup> they have crucial issues of the difficulty in making a smooth solid/solid interface between electrode and electrolyte, and chemical instability in contact with most of the electrode materials. This situation has focused renewed attention on organic electrolytes, and triggers both fundamental and applied research to develop undiscovered functions in organic electrolytes.

There are numerous organic solvents with diverse characteristics used in the area of chemistry. However, the organic electrolyte for lithium-ion batteries has almost no other option but ethylene carbonate (EC) based mixed solvents. This is because a graphite electrode, the most popular negative electrode in lithium-ion batteries, works reversibly only in the presence of EC solvent; an EC-based electrolyte allows for reversible lithium intercalation into a graphite electrode,<sup>12</sup>

**Special Issue:** New Materials and Approaches for Electrochemical Storage

**Received:** January 7, 2014

**Accepted:** March 13, 2014

**Published:** March 26, 2014

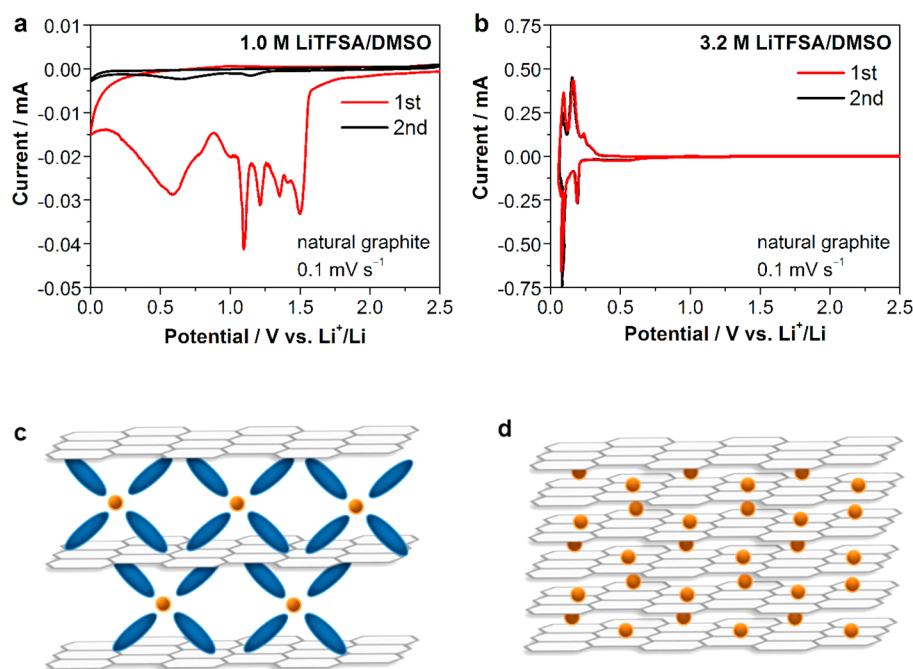


**Figure 1.** Cyclic voltammograms of natural graphite in (a) 1.0 mol dm<sup>-3</sup> and (b) 3.2 mol dm<sup>-3</sup> LiTFSA/DMSO electrolytes. Images of (c) solvent cointercalation (i.e., intercalation of solvated Li<sup>+</sup>) and (d) Li<sup>+</sup> intercalation.

whereas ethers (e.g., tetrahydrofuran (THF)), sulfoxides (e.g., dimethyl sulfoxide (DMSO)), or other organic carbonates (e.g., propylene carbonate (PC)) easily destroy the layered structure of graphite by severe electrolyte decompositions accompanied with cointercalation of solvent and lithium ion (i.e., intercalation of solvated lithium ion).<sup>13–16</sup> Because of the limitation of solvent compositions, there has been little advance in the organic electrolyte during the past two decades after the commercialization of lithium-ion batteries.

Recently, we and our collaborative group have proposed salt-superconcentrated organic solutions (e.g., >3 mol dm<sup>-3</sup> concentration) as an electrolyte for lithium-ion batteries.<sup>17–20</sup> A graphite electrode exhibits totally different behavior in a superconcentrated electrolyte; for example, a superconcentrated electrolyte of PC or DMSO suppresses the cointercalation of solvent to allow for reversible lithium intercalation into the interlayer of a graphite electrode.<sup>18,19</sup> Such previous results motivated us to propose the salt-superconcentrating strategy as a simple and effective approach for universalizing the graphite electrode reaction in various organic solvents other than EC.

In the present work, we demonstrate the universalization of reversible lithium intercalation into a graphite electrode in superconcentrated electrolytes composed of various organic solvent groups: ether, sulfoxide, and sulfone. Herein we used LiN(SO<sub>2</sub>CF<sub>3</sub>)<sub>2</sub> (LiTFSA, lithium bis-(trifluoromethanesulfonyl)amide) as a lithium salt, because it is easy to dissociate and dissolve in various organic solvents due to delocalized negative charge in the large anion. The molar concentration of the superconcentrated electrolytes in the present work is ca. 3 mol dm<sup>-3</sup>, which corresponds to the salt:solvent molar ratio of ca. 1:2. Following our previous study on a DMSO system,<sup>19</sup> we further discuss the origin of reversible lithium intercalation into a graphite electrode in superconcentrated electrolytes from the viewpoint of a surface film composition on the graphite and a coordination structure of lithium ion, anion, and solvent in a bulk solution.

## EXPERIMENTAL SECTION

**Materials.** All solvents and LiTFSA salt were purchased from Kishida Chemical Co. Ltd. The reagents were all lithium-battery grade (the water content is guaranteed below 20 ppm) and used without further purification. Superconcentrated solutions were prepared by adding a given amount of LiTFSA salt to a pure solvent with mild stirring and heating in an argon-filled glovebox. The molar concentration is defined as the molar amount of LiTFSA salt divided by the volume of the “whole solution” (not solvent only) in accordance with IUPAC.<sup>21</sup> Natural graphite powders (mean particle size: 10 μm) were provided by SEC Carbon, Ltd. and used without any pretreatment.

**Electrochemical Measurements.** A natural graphite electrode was prepared by mixing 90 wt % natural graphite powder and 10 wt % polyvinylidene difluoride (PVdF, Kureha Corporation) in *N*-methylpyrrolidone (NMP, Wako Pure Chemical Industries, Ltd.). The slurry was uniformly spread onto a copper current collector (10 μm thickness) with a 50 μm doctor blade and dried at 120 °C under vacuum overnight. The active material loading was ca. 1 mg cm<sup>-2</sup>. The obtained sheets were punched out to form a 16 mmφ disk electrode. Charge–discharge tests were carried out at 25 °C with a charge–discharge unit (TOSCAT, Toyo System Co., Ltd. or HJ1001SD8, Hokuto Denko Corporation) using a 2032-type coin cell with a lithium metal negative electrode and a glass fiber separator (Whatman GF/F, 420 mm thickness).

**Characterization.** To study the structural change of the natural graphite electrode, X-ray diffraction (XRD) patterns were obtained *ex situ* with a Bruker AXS D8 ADVANCE powder diffractometer (CoKα radiation) and a Vantec-1 linear position-sensitive detector. The 2θ value in the figure was converted to the one obtained by CuKα radiation. Surface chemistry of the natural graphite electrode was studied by X-ray photoelectron spectroscopy (XPS) using PHI 5000 VersaProbe (ULVAC-PHI, Inc.) equipped with a monochromatized AlKα X-ray Source. To prevent the air exposure of the graphite electrode, all the measurements were conducted under pure Ar atmosphere. Curve fitting of the spectra was performed with Gaussian–Lorentzian function after a Shirley-type background subtraction. Peaks were assigned based on previous reports.<sup>22–26</sup> To study the coordination structure in the solution, Raman spectra of the solutions were recorded with NRS-1000 (JASCO Corporation) using

an exciting laser of 514 nm. To prevent any contamination from air, we put the solution into a quartz cell and tightly sealed it in an argon-filled glovebox. The laser was radiated through the quartz crystal window.

## RESULTS AND DISCUSSION

**1. Lithium Intercalation into Graphite in DMSO.** First we show electrochemical behavior of natural graphite in DMSO solvent. DMSO is one of the most used solvents in various fields of chemistry because of its high dielectric constant, low toxicity, low volatility, and low price, but has not found wide application in batteries. This is because a graphite electrode, the most popular negative electrode, does not work reversibly in a DMSO electrolyte. Figure 1 shows cyclic voltammograms of a natural graphite electrode in conventional dilute  $1.0 \text{ mol dm}^{-3}$  and superconcentrated  $3.2 \text{ mol dm}^{-3}$  LiTfSA/DMSO electrolytes at  $25^\circ\text{C}$ . The electrochemical behavior of natural graphite was totally different in the two electrolytes. In the dilute  $1.0 \text{ mol dm}^{-3}$  LiTfSA/DMSO electrolyte, cathodic current was observed in a wide potential range from 1.5 to 0 V without a corresponding anodic peak, suggesting that the reaction is totally irreversible. In the previous work, the cathodic peaks in a range from 1.5 to 1.0 V are identified to be the cointercalation of lithium ion and DMSO solvent (i.e., intercalation of solvated  $\text{Li}^+(\text{DMSO})_x$ ) into the interlayer of graphite.<sup>27</sup> The cathodic peaks below 1.0 V indicate that the cointercalated  $\text{Li}^+(\text{DMSO})_x$  suffered from reductive decompositions in the interlayer of graphite to destroy the layered structure. Due to the solvent cointercalation followed by reductive decompositions, a graphite electrode does not work reversibly in a conventional dilute DMSO electrolyte. On the other hand, in the superconcentrated  $3.2 \text{ mol dm}^{-3}$  LiTfSA/DMSO electrolyte, no broad cathodic peaks were observed in a range of 1.5 to 1.0 V, indicating that the intercalation of solvated  $\text{Li}^+(\text{DMSO})_x$  was fully suppressed in the superconcentrated solution. Instead, we observed a reversible redox pair in the vicinity of 0 V. The ex situ XPD pattern (Figure 2) of the graphite at 0.03 V showed

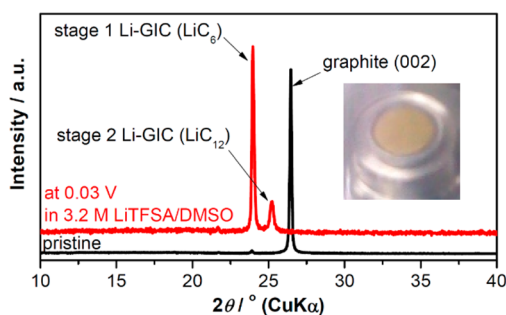


**Figure 2.** XRD pattern of the graphite electrode kept at 0.03 V in  $3.2 \text{ mol dm}^{-3}$  LiTfSA/DMSO electrolyte. Inset is the image of the electrode.

the (001) peak of stage 1 lithium-graphite intercalation compound (Li-GIC) ( $\text{LiC}_6$ ) with interlayer distance of 0.371 nm and the small peak of stage 2 Li-GIC ( $\text{LiC}_{12}$ ),<sup>28,29</sup> where the graphite electrode turned gold (Figure 2, inset). On the basis of these results, it is evident that the superconcentrated DMSO electrolyte allows for lithium intercalation into a graphite electrode by suppressing solvent cointercalation. Note that the experiment was conducted under a severe condition, where we did not rely on any techniques to facilitate reversible lithium intercalation such as the surface treatment of natural

graphite<sup>30</sup> and the use of functional binders<sup>31</sup> or electrolyte additives.<sup>32–34</sup> The totally different behavior of a natural graphite electrode should primarily arise from a peculiar bulk/interfacial nature of superconcentrated electrolytes, as discussed below.

**2. Bulk Solution Structure.** To identify the solution structure providing such unusual electrochemical behavior, we measured Raman spectra (Figure 3) for LiTfSA/DMSO solutions at various lithium-salt concentrations. The Raman spectrum of pure DMSO in Figure 3a shows two bands at  $671$  and  $701 \text{ cm}^{-1}$ , which arise from C–S symmetric and asymmetric stretching mode of free DMSO (i.e., without coordinating to  $\text{Li}^+$ ).<sup>35–37</sup> In the dilute  $1.0 \text{ mol dm}^{-3}$  LiTfSA/DMSO solution, small peaks appear at  $679$  and  $713 \text{ cm}^{-1}$ , which are attributed to C–S symmetric and asymmetric stretching mode of  $\text{Li}^+$ -solvating DMSO.<sup>36,37</sup> Hence, both free and solvating DMSO molecules exist in such a dilute solution. In general, a stable solvation structure around  $\text{Li}^+$  is considered to be 4-fold coordination (Figure 3b)<sup>38–42</sup> and the stable  $\text{Li}^+(\text{DMSO})_4$  solvate should intercalate into graphite without desolvation to form a ternary Li-DMSO-GIC in a dilute DMSO electrolyte. On the other hand, in the superconcentrated  $3.2 \text{ mol dm}^{-3}$  LiTfSA/DMSO solution, which allows for reversible lithium intercalation into graphite, there are only peaks for  $\text{Li}^+$ -solvating DMSO, suggesting that all DMSO molecules coordinate to  $\text{Li}^+$  and there is no free DMSO in the superconcentrated solution. Since the molar ratio of LiTfSA:DMSO is ca. 1:2 in  $3.2 \text{ mol dm}^{-3}$  LiTfSA/DMSO, lithium ions are forced to have unstable 2-fold DMSO coordination on average (Figure 3b). Because of the scarcity of DMSO solvents, there are few stable solvate (i.e.,  $\text{Li}^+(\text{DMSO})_4$ ), which can easily form the ternary Li-DMSO-GIC. We postulate that the 2-fold coordination solvate (i.e.,  $\text{Li}^+(\text{DMSO})_2$ ) is too unstable to exist in the interlayer of graphite and hence cannot form the ternary Li-DMSO-GIC. This is why the solvent cointercalation is suppressed in the superconcentrated electrolyte.

Next, the Raman band in Figure 3a show S–N stretching, C–S stretching, and  $\text{CF}_3$  bending modes of TfSA<sup>−</sup> anion.<sup>41</sup> It is clear that the Raman band shifts to high wavenumber in the superconcentrated  $3.2 \text{ mol dm}^{-3}$  LiTfSA/DMSO solution. The upshift of the Raman band arises from the presence of Coulombic interaction between TfSA<sup>−</sup> and  $\text{Li}^+$ ;<sup>41</sup> there should be considerable amount of contact ion pairs (CIPs, a pair of one TfSA<sup>−</sup> and one  $\text{Li}^+$ ) and aggregates (AGGs, TfSA<sup>−</sup> coordinating to two or more  $\text{Li}^+$  cations) because of the relative scarcity of DMSO solvents. We consider that the presence of strong Coulombic interaction should be another factor to suppress the intercalation of solvated  $\text{Li}^+$  into graphite. The series of Raman analyses suggest that in the superconcentrated  $3.2 \text{ mol dm}^{-3}$  LiTfSA/DMSO solution, all TfSA<sup>−</sup> anions and DMSO solvents coordinate to  $\text{Li}^+$  to form a polymeric fluid network of  $\text{Li}^+$  and TfSA<sup>−</sup>. This unique solution structure gives rise to the peculiar electrochemical behavior of a graphite electrode.

**3. Surface Film.** A surface film, referred to as solid electrolyte interphase (SEI),<sup>43</sup> is a key to reversible lithium-ion intercalation into a graphite electrode.<sup>44,45</sup> It is well-known that EC solvent is reduced to form a stable SEI on the surface of graphite during first charge ( $\text{Li}^+$  intercalation), which suppresses further reductive decompositions of the electrolyte. This is why a graphite negative electrode works reversibly in an EC-based electrolyte. In the present cases, however, there are



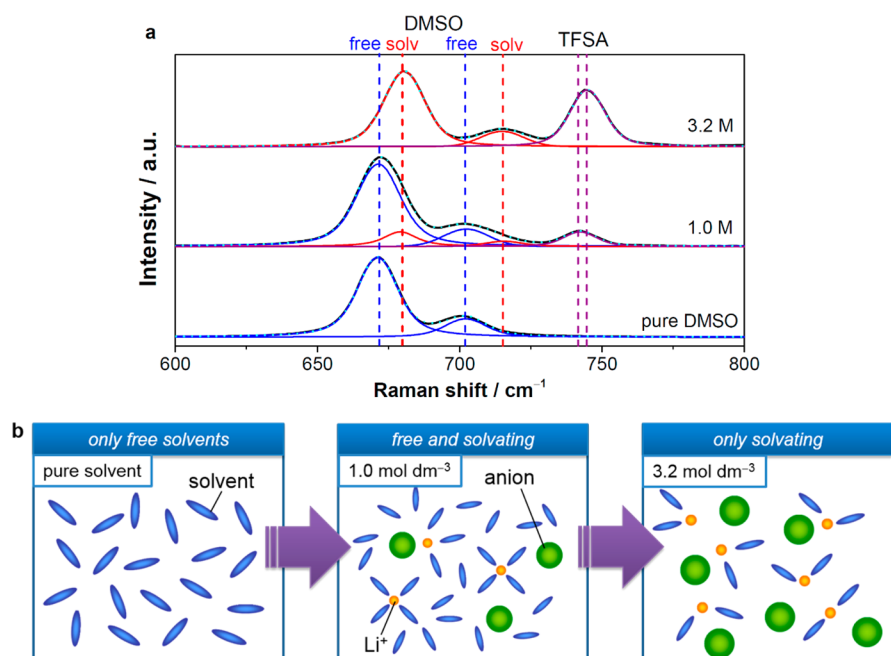


**Figure 3.** (a) Raman spectra of LiTFSA/DMSO solutions at various salt concentrations. (b) Schematic of coordination structure in dilute and superconcentrated solutions.

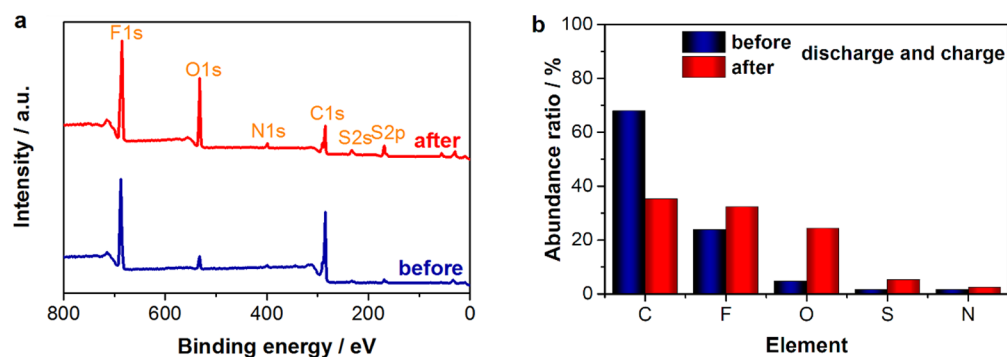


**Figure 4.** (a) Wide-scan XPS spectra and (b) surface atomic ratio on the natural graphite electrode before and after one-cycle charge and discharge in  $3.2 \text{ mol dm}^{-3}$  LiTFSA/DMSO electrolyte at  $C/10$  rate.

no film-forming solvents like EC or vinylene carbonate in the electrolyte, but the graphite electrode works reversibly without severe electrolyte decompositions. This apparently contradictory result motivated us to study the surface film composition in the superconcentrated DMSO electrolyte.

Figure 4 shows XPS profiles for the natural graphite electrode before and after a charge–discharge test in superconcentrated  $3.2 \text{ mol dm}^{-3}$  LiTFSA/DMSO electrolyte. Before a charge–discharge test (i.e., just immersed in the electrolyte for 24 h and washed with dimethyl carbonate (DMC)), the major surface element was C deriving from the natural graphite. A small amount of F element also existed on the surface, which should derive from the PVdF binder and residual LiTFSA salt. The amount of S and N elements was quite low, suggesting that residual LiTFSA salt was negligible after the wash with DMC. On the other hand, after one-cycle discharge and charge in the superconcentrated DMSO electrolyte, the amount of C remarkably decreased and the other elements F and O became the main surface components with non-negligible presence of S and N elements. This indicates that the surface of the graphite

electrode was covered with an SEI film rich in F and O elements.

To further obtain information on the SEI compositions, a detailed analysis was made on the spectra of main components, C 1s, O 1s, and F 1s (Figure 5). In the C 1s spectrum (Figure 5a), a small amount of graphite (i.e.,  $\text{sp}^2\text{-C}$ ) was observed on the electrode surface, suggesting the presence of a SEI film covering the graphite. The  $\text{sp}^3\text{-C}$ , C–O,  $\text{CO}_3$ , and  $\text{CF}_3$  components should arise from the SEI film and/or the surface functional groups on the graphite. From the O 1s spectrum (Figure 5b), we could not identify the accurate chemical states of O element, because several chemical states containing S and/or C give almost the same binding energies at around 532 eV. On the other hand, the F 1s spectrum shows that the major F component is LiF with a small amount of residual LiTFSA salt (i.e.,  $\text{CF}_3$ ) and PVdF binder (Figure 5c). Since LiF should arise from the decomposition of TFSA anions, the TFSA anions largely contribute to the SEI formation process. At present, the contribution of DMSO solvents to the SEI formation is not clear, but it is true that the SEI film is rich in F and O elements due to the preferential decomposition of TFSA anions. We

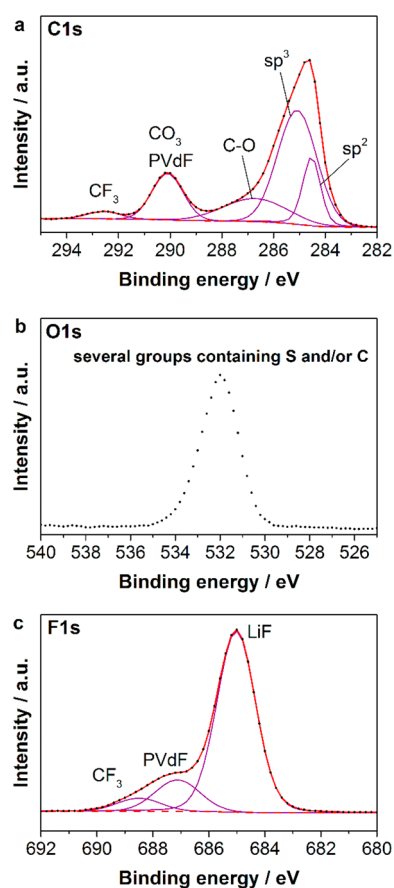


**Figure 5.** (a) C 1s, (b) O 1s, and (c) F 1s spectra of the natural graphite electrode cycled in 3.2 mol dm<sup>-3</sup> LiTFSA/DMSO electrolyte. Points and solid lines denote experimental spectra and fitting curves, respectively.

consider that the superconcentrated solutions facilitate the reductive decomposition of TFSA anions to form a TFSA-based inorganic SEI film, which effectively suppresses further reductive decomposition of the electrolyte. The detailed mechanism is outside the scope of this paper and will be reported elsewhere.

**4. Universal Observation of Lithium Intercalation into Graphite.** Having confirmed the unique bulk/interfacial features of a superconcentrated DMSO electrolyte, we studied charge–discharge behavior of natural graphite/lithium metal half cell with various dilute and superconcentrated organic electrolytes (Figure 6). In all cases, the natural graphite electrode does not work reversibly in dilute electrolytes without EC solvent. For example, in a dilute DMSO electrolyte (Figure 6a), the voltage was kept constant over 0.8 V, where the destruction of graphite as well as solvent cointercalation and electrolyte decompositions occurred, which is consistent with the result of cyclic voltammetry (Figure 1). In dilute LiTFSA/SL and LiTFSA/THF electrolytes (Figure 6c, e), large irreversible capacity was observed with a voltage plateau at around 0.5 V at which lithium intercalation does not occur. The dilute LiTFSA/SL electrolyte also resulted in a voltage plateau at near 0 V, which was larger than the theoretical capacity of lithium intercalation into graphite (372 mAh g<sup>-1</sup>). The large irreversible capacity is attributed to reductive decompositions of the electrolyte. The decomposition products do not work as a good SEI film that can suppress further reductive decom-

positions of the electrolyte and thus, the reversibility of a graphite electrode is poor in the dilute electrolytes without EC solvent. On the other hand, all the superconcentrated electrolytes of DMSO, SL, and THF (Figure 5b, d, f) resulted in highly reversible discharge and charge curves with around 300 mAh g<sup>-1</sup>, which is close to the theoretical capacity of graphite (372 mAh g<sup>-1</sup>). The voltage curves showed several plateaus below 0.5 V, which are characteristic of the formation of several stage structures of Li-GIC.<sup>28,29</sup> The superconcentrated electrolytes allow for reversible lithium intercalation and deintercalation at a natural graphite electrode even in the absence of the film-forming EC solvent, suppressing continuous electrolyte decomposition and solvent cointercalation destroying the layered structure of graphite. It is also interesting to note the different irreversible capacities in first cycle depending on the solvents; the irreversible capacity becomes large in such solvents prone to cointercalation (e.g., DMSO) even at a superhigh concentration. This suggests a competitive reaction of solvent cointercalation and film formation (i.e., decomposition of TFSA anion) in first cycle in which the formation of stable SEI film is incomplete.

The totally different behavior of a graphite electrode in superconcentrated electrolytes should in common arise from the unique bulk/interfacial features of superconcentrated electrolytes. First, superconcentrated electrolytes have totally different solution structure from those of conventional dilute ones; the low solvation number to Li<sup>+</sup> and the formation of ion pairs (CIPs and AGGs) should be a factor to suppress the solvent cointercalation to allow for reversible Li<sup>+</sup> intercalation. Second, the SEI-forming ability is modified at superhigh concentrations; TFSA anions contribute largely to SEI formation on the surface of graphite, which should be another reason for efficient cycling of graphite electrode even in the absence of film forming solvents. However, the nature of the TFSA-based SEI contributing to reversible Li<sup>+</sup> intercalation is not clear at present. Further considerations are needed for the SEI-formation mechanism, including comparative studies on superconcentrated electrolytes with other salts (e.g., LiPF<sub>6</sub>, LiClO<sub>4</sub>, and LiBF<sub>4</sub>), and also for the Li<sup>+</sup> intercalation mechanism accompanied with decomplexation of CIPs and AGGs.

Our salt-superconcentrating strategy expands the graphite negative electrode reaction for a wide variety of organic solvents other than EC. This breakthrough defies the long-believed conventional notion that lithium-ion batteries operate only with an EC-based electrolyte, and opens up the way to advanced lithium-ion batteries based on various EC-free organic electrolytes with diverse characteristics. For example, a superconcentrated solution of oxidation tolerant solvents (e.g., SL and acetonitrile) will be a promising electrolyte for high-voltage lithium-ion batteries employing a 5 V-class positive electrode and a graphite negative electrode, which do not work reversibly in a conventional EC-based electrolyte due to its poor oxidative stability. Furthermore, we recently reported outstanding lithium intercalation kinetics in a superconcentrated ether electrolyte, even exceeding that in a currently used commercial EC-based electrolyte.<sup>20</sup> Hence, the superconcentrated electrolyte will also have the possibility of realizing fast-charging lithium-ion batteries, which are urgently required for automobile applications. Although there are some problems to be overcome (e.g., irreversible capacity at first cycle and aluminum corrosion by TFSA anions) and there should be a long way to realize a superconcentrated electrolyte in

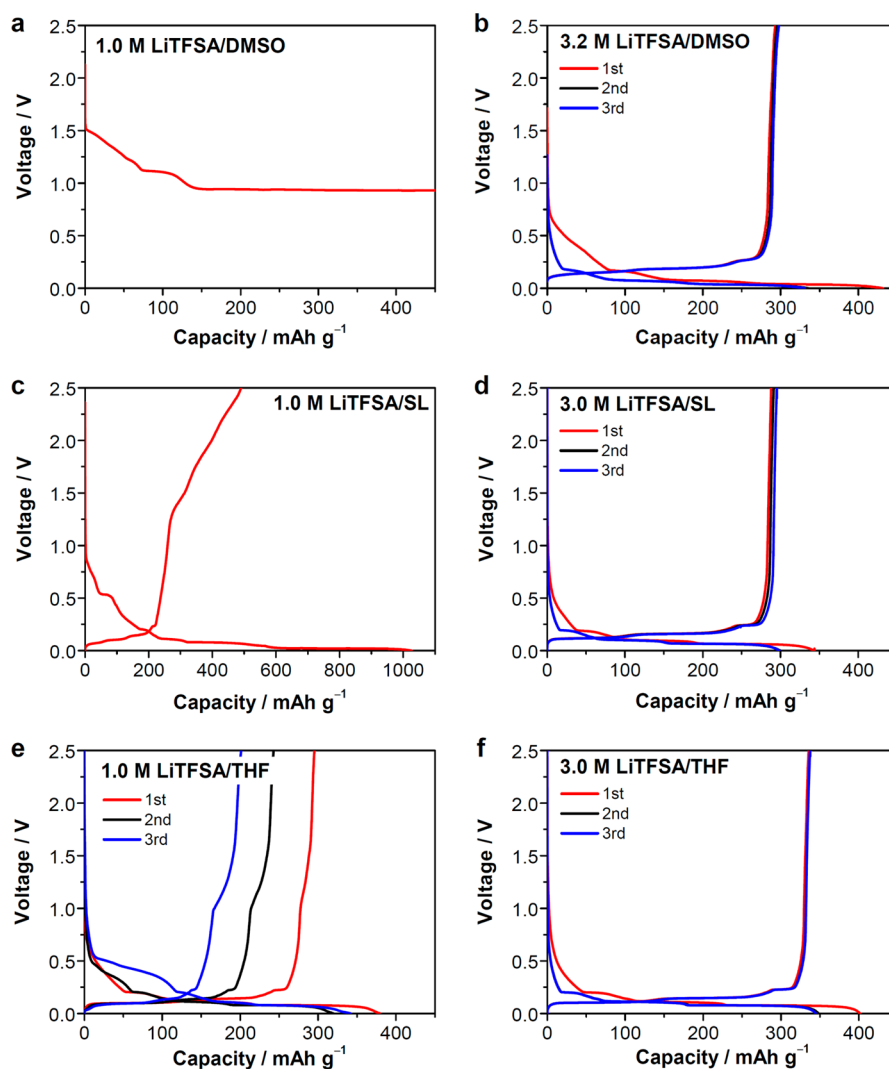


**Figure 6.** Charge–discharge curves of natural graphite/lithium metal half cell with (a) 1.0 and (b) 3.2 mol dm<sup>-3</sup> LiTfSA/DMSO, (c) 1.0 and (d) 3.0 mol dm<sup>-3</sup> LiTfSA/SL, and (e) 1.0 and (f) 3.0 mol dm<sup>-3</sup> LiTfSA/THF electrolytes at a C/10 rate.

commercial advanced batteries, we believe that the universal operation of a graphite negative electrode in various superconcentrated electrolytes will be an important breakthrough toward the diversification of organic electrolyte with various required functions to realize advanced lithium-ion batteries.

## CONCLUSIONS

We have presented a salt-superconcentrating strategy as a simple and effective method for universalizing a graphite negative electrode reaction in various organic solvents without EC. A superconcentrated electrolyte (e.g., >3 mol dm<sup>-3</sup>) of sulfoxide, ether, or sulfone allows for highly reversible lithium intercalation into a graphite electrode, whereas in conventional dilute electrolytes (e.g., 1 mol dm<sup>-3</sup>) without EC or other film-forming additives, solvent cointercalation and/or severe reductive decomposition occur to hamper reversible lithium intercalation. The superconcentrated electrolytes have unique solution structure with ion pair and small solvation number in the absence of free (uncoordinating) solvents, and form an anion-based inorganic SEI film on the surface of a graphite negative electrode. The anion-based SEI as well as unique solution structure should be the origin of the universal working of a graphite negative electrode in various superconcentrated

electrolytes. Our salt-superconcentrating strategy, universalizing a graphite negative electrolyte reaction in various organic solvents, will allow us to design new EC-free functional electrolytes with various organic solvents with diverse characteristics, which will be an important step toward next-generation advanced lithium-ion batteries with high-voltage and fast-charging characteristics.

## AUTHOR INFORMATION

### Corresponding Author

\*E-mail: yamada@chemsys.t.u-tokyo.ac.jp.

### Notes

The authors declare no competing financial interest.

## ACKNOWLEDGMENTS

This work was partially supported by Advanced Low Carbon Technology Research and Development Program (ALCA) of Japan Science and Technology Agency (JST) and JSPS KAKENHI Grant number 23750211.

## REFERENCES

- (1) Tarascon, J.-M.; Armand, M. Issues and Challenges Facing Rechargeable Lithium Batteries. *Nature* **2001**, *414*, 359–367.

- (2) Armand, M.; Tarascon, J.-M. Building Better Batteries. *Nature* **2008**, *451*, 652–657.
- (3) Goodenough, J. B.; Kim, Y. Challenges for Rechargeable Li Batteries. *Chem. Mater.* **2010**, *22*, 587–603.
- (4) Bruce, P. G.; Freunberger, S. A.; Hardwick, L. J.; Tarascon, J.-M. Li–O<sub>2</sub> and Li–S Batteries with High Energy Storage. *Nat. Mater.* **2012**, *11*, 19–29.
- (5) Armand, M.; Endres, F.; MacFarlane, D. R.; Ohno, H.; Scrosati, B. Ionic-Liquid Materials for the Electrochemical Challenges of the Future. *Nat. Mater.* **2009**, *8*, 621–629.
- (6) Galinski, M.; Lewandowski, A.; Stepniak, I. Ionic Liquids As Electrolytes. *Electrochim. Acta* **2006**, *51*, 5567–5580.
- (7) Sakaebe, H.; Matsumoto, H. *N*-Methyl-*N*-propylpiperidinium Bis(Trifluoromethanesulfonyl) Imide (PP13-TFSI)—Novel Electrolyte Base for Li Battery. *Electrochem. Commun.* **2003**, *5*, 594–598.
- (8) Yoon, H.; Howlett, P. C.; Best, A. S.; MacFarlane, D. R. Fast Charge/Discharge of Li Metal Batteries Using an Ionic Liquid Electrolyte. *J. Electrochem. Soc.* **2013**, *160*, A1629–A1637.
- (9) Kamaya, N.; Homma, K.; Yamakawa, Y.; Hirayama, M.; Kanno, R.; Yonemura, M.; Kamiyama, T.; Kato, Y.; Hama, S.; Kawamoto, K.; Mitsui, A. A Lithium Superionic Conductor. *Nat. Mater.* **2011**, *10*, 682–686.
- (10) Inaguma, Y.; Chen, L.; Itoh, M.; Nakamura, T. High Ionic Conductivity in Lithium Lanthanum Titanate. *Solid State Commun.* **1993**, *86*, 689–693.
- (11) Mizuno, F.; Hayashi, A.; Tadanaga, K.; Tatsumisago, M. High Lithium Ion Conducting Glass-Ceramics in the System Li<sub>2</sub>S–P<sub>2</sub>S<sub>5</sub>. *Solid State Ionics* **2006**, *177*, 2721–2725.
- (12) Ikeda, H.; Narukawa, S.; Nakajima, H. *Jp. Pat.* **1981**, 176966.
- (13) Dey, A. N.; Sullivan, B. P. The Electrochemical Decomposition of Propylene Carbonate on Graphite. *J. Electrochem. Soc.* **1970**, *117*, 222–224.
- (14) Besenhard, J. O. The Electrochemical Preparation and Properties of Ionic Alkali Metal- and NR<sub>4</sub>-Graphite Intercalation Compounds in Organic Electrolytes. *Carbon* **1976**, *14*, 111–115.
- (15) Aurbach, D.; Levi, M. D.; Levi, E.; Schechter, A.; Granot, E. Recent Studies on the Correlation between Surface Chemistry, Morphology, Three-Dimensional Structures and Performance of Li and Li-C Intercalation Anodes in Several Important Electrolyte Systems. *J. Power Sources* **1997**, *68*, 91–98.
- (16) Abe, T.; Kawabata, N.; Mizutani, Y.; Inaba, M.; Ogumi, Z. Correlation between Cointercalation of Solvents and Electrochemical Intercalation of Lithium into Graphite in Propylene Carbonate Solution. *J. Electrochem. Soc.* **2003**, *150*, A257–A261.
- (17) Jeong, S.-K.; Seo, H.-Y.; Kim, D.-H.; Han, H.-K.; Kim, J.-G.; Lee, Y. B.; Iriyama, Y.; Abe, T.; Ogumi, Z. Suppression of Dendritic Lithium Formation by Using Concentrated Electrolyte Solutions. *Electrochem. Commun.* **2008**, *10*, 635–638.
- (18) Jeong, S.-K.; Inaba, M.; Iriyama, Y.; Abe, T.; Ogumi, Z. Electrochemical Intercalation of Lithium Ion within Graphite from Propylene Carbonate Solutions. *Electrochem. Solid-State Lett.* **2003**, *6*, A13–A15.
- (19) Yamada, Y.; Takazawa, Y.; Miyazaki, K.; Abe, T. Electrochemical Lithium Intercalation into Graphite in Dimethyl Sulfoxide-Based Electrolytes: Effect of Solvation Structure of Lithium Ion. *J. Phys. Chem. C* **2010**, *114*, 11680–11685.
- (20) Yamada, Y.; Yaegashi, M.; Abe, T.; Yamada, A. A Superconcentrated Ether Electrolyte for Fast-Charging Li-Ion Batteries. *Chem. Commun.* **2013**, *49*, 11194–11196.
- (21) IUPAC. *Quantities, Units and Symbols in Physical Chemistry*, 3rd ed; RSC Publishing: London, 2007.
- (22) Verma, P.; Maire, P.; Novák, P. A Review of the Features and Analyses of the Solid Electrolyte Interphase in Li-Ion Batteries. *Electrochim. Acta* **2010**, *55*, 6332–6341.
- (23) Leroy, S.; Martinez, H.; Dedryvère, R.; Lemordant, D.; Gonbeau, D. Influence of the Lithium Salt Nature over the Surface Film Formation on a Graphite Electrode in Li-Ion Batteries: An XPS Study. *Appl. Surf. Sci.* **2007**, *253*, 4895–4905.
- (24) Diaz, J.; Paolicelli, G.; Ferrer, S.; Comin, F. Separation of the sp<sup>3</sup> and sp<sup>2</sup> Components in the C 1s Photoemission Spectra of Amorphous Carbon Films. *Phys. Rev. B* **1996**, *54*, 8064–8069.
- (25) Leroy, S.; Blanchard, F.; Dedryvère, R.; Martinez, H.; Carré, B.; Lemordant, D.; Gonbeau, D. Surface Film Formation on a Graphite Electrode in Li-Ion Batteries: AFM and XPS Study. *Surf. Interface Anal.* **2005**, *37*, 773–781.
- (26) Ensling, D.; Stjernedahl, M.; Nyttén, A.; Gustafsson, T.; Thomas, J. O. A Comparative XPS Surface Study of Li<sub>2</sub>FeSiO<sub>4</sub>/C Cycled with LiTFSI- and LiPF<sub>6</sub>-Based Electrolytes. *J. Mater. Chem.* **2009**, *19*, 82–88.
- (27) Abe, T.; Fukuda, H.; Iriyama, Y.; Ogumi, Z. Solvated Li-Ion Transfer at Interface between Graphite and Electrolyte. *J. Electrochem. Soc.* **2004**, *151*, A1120–A1123.
- (28) Dahn, J. R. Phase Diagram of Li<sub>x</sub>C<sub>6</sub>. *Phys. Rev. B* **1991**, *44*, 9170–9177.
- (29) Ohzuku, T.; Iwakoshi, Y.; Sawai, K. Formation of Lithium-Graphite Intercalation Compounds in Nonaqueous Electrolytes and Their Application As a Negative Electrode for a Lithium Ion (Shuttlecock) Cell. *J. Electrochem. Soc.* **1993**, *140*, 2490–2498.
- (30) Wu, Y. P.; Jiang, C.; Wan, C.; Holze, R. Anode Materials for Lithium Ion Batteries by Oxidative Treatment of Common Natural Graphite. *Solid State Ionics* **2003**, *156*, 283–290.
- (31) Komaba, S.; Ozeki, T.; Okushi, K. Functional Interface of Polymer Modified Graphite Anode. *J. Power Sources* **2009**, *189*, 197–203.
- (32) Wrodnigg, G. H.; Besenhard, J. O.; Winter, M. Ethylene Sulfite As Electrolyte Additive for Lithium-Ion Cells with Graphitic Anodes. *J. Electrochem. Soc.* **1999**, *146*, 470–472.
- (33) Aurbach, D.; Bamolsky, K.; Markovsky, B.; Gofer, Y.; Schmidt, M.; Heider, U. On the Use of Vinylene Carbonate (VC) as an Additive to Electrolyte Solutions for Li-Ion Batteries. *Electrochim. Acta* **2002**, *47*, 1423–1439.
- (34) Zhang, S. S. A Review on Electrolyte Additives for Lithium-Ion Batteries. *J. Power Sources* **2006**, *162*, 1379–1394.
- (35) Emons, H. H.; Birkeneder, F.; Pollmer, K. Studies on Systems of Salts and Mixed Solvents. XXXIII. On the Solvation of Cations (Li<sup>+</sup>, Mg<sup>2+</sup>, Al<sup>3+</sup>) in Dimethylsulphoxide-Water Mixtures (Raman Spectroscopic Investigations into Concentrated Electrolyte Solutions). *Z. Anorg. Allg. Chem.* **1986**, *534*, 175–187.
- (36) Alia, J. M.; Edwards, H. G. M. Ion Solvation and Ion Association in Lithium Trifluoromethanesulfonate Solutions in Three Aprotic Solvents. An FT-Raman Spectroscopic Study. *Vib. Spectrosc.* **2000**, *24*, 185–200.
- (37) Xuan, X. P.; Wang, J. J.; Zhao, Y.; Zhu, J. J. Experimental and Computational Studies on the Solvation of Lithium Tetrafluoroborate in Dimethyl Sulfoxide. *J. Raman Spectrosc.* **2007**, *38*, 865–872.
- (38) Hyodo, S.; Okabayashi, K. Raman Intensity Study of Local Structure in Non-Aqueous Electrolyte Solutions— I. Cation–Solvent Interaction in LiClO<sub>4</sub>/Ethylene Carbonate. *Electrochim. Acta* **1989**, *34*, 1551–1556.
- (39) Morita, M.; Asai, Y.; Yoshimoto, N.; Ishikawa, M. A Raman Spectroscopic Study of Organic Electrolyte Solutions Based on Binary Solvent Systems of Ethylene Carbonate with Low Viscosity Solvents Which Dissolve Different Lithium Salts. *J. Chem. Soc., Faraday Trans.* **1998**, *94*, 3451–3456.
- (40) Deng, Z.; Irish, D. E. Raman spectral studies of ion association and solvation in solutions of LiAsF<sub>6</sub>-acetone. *J. Chem. Soc., Faraday Trans.* **1992**, *88*, 2891–2896.
- (41) Seo, D. M.; Borodin, O.; Han, S.-D.; Boyle, P. D.; Henderson, W. A. Electrolyte Solvation and Ionic Association II. Acetonitrile–Lithium Salt Mixtures: Highly Dissociated Salts. *J. Electrochem. Soc.* **2012**, *159*, A1489–A1500.
- (42) Seo, D. M.; Boyle, P. D.; Borodin, O.; Henderson, W. A. Li<sup>+</sup> Cation Coordination by Acetonitrile—Insights from Crystallography. *RSC Adv.* **2012**, *2*, 8014–8019.
- (43) Peled, E. The Electrochemical Behavior of Alkali and Alkaline Earth Metals in Nonaqueous Battery Systems—The Solid Electrolyte Interphase Model. *J. Electrochem. Soc.* **1979**, *126*, 2047–2051.

(44) Aurbach, D. Review of Selected Electrode-Solution Interactions Which Determine the Performance of Li and Li Ion Batteries. *J. Power Sources* **2000**, *89*, 206–218.

(45) Yazami, R. Surface Chemistry and Lithium Storage Capability of the Graphite-Lithium Electrode. *Electrochim. Acta* **1999**, *45*, 87–97.